

**Effects of the density-dependent weak form factors on the  
neutrino reaction via neutral current for the nucleon in nuclear  
matter and  $^{12}\text{C}$**

Myung-Ki Cheoun,<sup>1,\*</sup> Ki-Seok Choi,<sup>1,†</sup> K. S. Kim,<sup>2,‡</sup> Koichi Saito,<sup>3,§</sup>  
Toshitaka Kajino,<sup>4,¶</sup> Kazuo Tsushima,<sup>5,6,\*\*</sup> and Tomoyuki Maruyama<sup>7,††</sup>

<sup>1</sup>*Department of Physics, Soongsil University, Seoul 156-743, Korea*

<sup>2</sup>*School of Liberal Arts and Science,*

*Korea Aerospace University, Koyang 412-791, Korea*

<sup>3</sup>*Department of Physics, Faculty of Science and Technology,*

*Tokyo University of Science, Noda 278-8510, Japan*

<sup>4</sup>*National Astronomical Observatory of Japan,*

*2-21-1 Osawa, Mitaka, Tokyo 181-8588, Japan*

*and Department of Astronomy, Graduate School of Science,*

*University of Tokyo, Hongo 7-3-1, Bunkyo-ku, Tokyo 113-0033, Japan*

<sup>5</sup>*CSSM, School of Chemistry and Physics,*

*University of Adelaide, Adelaide SA 5005, Australia*

<sup>6</sup>*International Institute of Physics (IIP),*

*Federal University of Rio Grande do Norte (UFRN), Natal/RN 59078-400, Brazil*

<sup>7</sup>*College of Bioresource Sciences, Nihon University, Fujisawa 252-8510, Japan*

(Dated: November 16, 2018)

## Abstract

The nucleon form factors in free space are usually thought to be modified when a nucleon is bound in a nucleus or immersed in a nuclear medium. We investigate effects of the density-dependent axial and weak-vector form factors on the electro-neutrino ( $\nu_e$ ) and anti-electro-neutrino ( $\bar{\nu}_e$ ) reactions with incident energy  $E_\nu \leq 80$  MeV via neutral current (NC) for a nucleon in a nuclear medium or  $^{12}\text{C}$ . For the density-dependent form factors, we exploit the quark-meson-coupling (QMC) model, and apply them to the  $\nu_e$  and  $\bar{\nu}_e$  induced reactions by NC. About 12 % decrease of the total cross section by the  $\nu_e$  reaction on the nucleon is obtained at normal density,  $\rho = \rho_0 \sim 0.15 \text{fm}^{-3}$ , as well as about 18 % reduction of the total  $\nu_e$  cross section on  $^{12}\text{C}$ , by the modification of the weak form factors of the bound nucleon.

However, similarly to the charged current reaction, effects of the nucleon property change in the  $\bar{\nu}_e$  reaction reduce significantly the cross sections about 30 % for the nucleon in matter and  $^{12}\text{C}$  cases. Such a large asymmetry in the  $\bar{\nu}_e$  cross sections is addressed to originate from the different helicities of  $\bar{\nu}_e$  and  $\nu_e$ .

PACS numbers: 14.20.Dh, 25.30.Pt, 26.30.-k, 26.30.Jk

---

\*cheoun@ssu.ac.kr

†kiseokchoi@gmail.com

‡kyungsik@kau.ac.kr

§koichi.saito@rs.tus.ac.jp

¶kajino@nao.ac.jp

\*\*kazuo.tsushima@gmail.com

††maruyama.tomoyuki@nihon-u.ac.jp

## I. INTRODUCTION

In the core-collapse supernova (SN) explosion, neutrino ( $\nu$ ) heating is known as one of the main mechanisms for the explosion leading to the so-called  $\nu$ -driven explosion [1]. Neutrinos emitted from the neutrino sphere propagate the proto-neutron star (PNS). The first propagating region is a core part of the PNS, whose density is believed to be about a few times of the normal nuclear density  $\rho_0 \sim 0.15 fm^{-3}$ . During the propagation, neutrinos may interact with nucleons in dense nuclear matter through two different modes; neutral current (NC) and charged current (CC). The former mediated by  $Z^0$  boson corresponds to the neutrino scattering, while the latter through  $W^\pm$  bosons is the neutrino absorption with the emission of corresponding leptons.

After passing by the uniform density region,  $\rho_{uni} \sim 6.85 \times 10^{-2} fm^{-3} = 1.14 \times 10^{14} g/cm^3 \sim 0.5\rho_o$ , which density dissolves a crust of the PNS into the core comprising a uniform plasma of nucleons and leptons, neutrinos enter into the crust region of the PNS. This crust region is usually treated as two different parts, inner and outer crusts divided by the neutron drip density,  $\rho_{drip} \sim 2.70 \times 10^{-4} fm^{-3} = 4.48 \times 10^{11} g/cm^3$ . Beyond this density, neutrons drip out of finite nuclei presumed to be embedded as lattice structures in the outer crust of the neutron star.

Some of the interesting phenomena in the  $\nu$  propagation inside the PNS by a unique property of the neutrino come from the asymmetry between the neutrino scattering and absorption due to strong magnetic fields in the magnetar. For instance, the pulsar kick [2, 3] and the spin deceleration [4] of the strongly magnetized neutron stars were shown to be closely associated with the asymmetry, according to detailed studies of the neutrino transport in dense matter by a relativistic mean field theory (RMF).

Outside of the PNS, emitted neutrinos interact also with the nuclei already produced by the s-process in the progenitor and/or the r-process in the explosion. Around the Si layer, the neutrinos may initiate the so called neutrino-proton ( $\nu p$ ) process [5]. Namely, the anti-neutrino ( $\bar{\nu}$ ) absorption in proton-rich environment may produce neutrons immediately captured by neutron-deficient nuclei, which affects the proton process (p-process) by the  $(n, p)$  or  $(n, \gamma)$  reactions. In the O-Ne-Mg layer, whose density is assumed to be about  $\rho \sim 10^3 g/cm^3$ , neutrino-induced reactions might play an important role of producing some p-nuclei, which are odd-odd neutron-deficient nuclei. For example, the cosmological origins

of  $^{180}\text{Ta}$  and  $^{138}\text{La}$  are believed to originate from the  $\nu$ -process [6, 7]. Other light nuclei abundances are also closely associated with the neutrino interactions in He-C layer [8].

Of course, the nuclear density outside the PNS is not so dense compared to that of inside the PNS. But, since the nucleons interacting with the neutrinos are strongly bound, properties of such a bound nucleon are expected to be modified from those in free space. Therefore, if such a drastic change of nuclear density happens to the neutrino propagation, it would be of practical importance to investigate such medium effects or bound nucleon property changes on the neutrino propagation in both inside and outside of the PNS.

Moreover, recently, strong evidences for the modification of the nucleon properties in a nuclear medium have been reported from the proton electromagnetic (EM) form factors measured in polarized  $(\vec{e}, e'\vec{p})$  scattering on  $^{16}\text{O}$  [9] and  $^4\text{He}$  [10–14] at MAMI and Jefferson Lab, and also from the study of neutron properties in a nuclear medium through polarized  $(\vec{e}, e'\vec{n})$  scattering on  $^4\text{He}$  in Ref. [15]. Since the weak vector currents and EM currents form iso-vector (vector) current, one may expect naturally the modification of the weak vector form factors in a similar way to the EM form factors. In addition, the fact that the bound neutron in a nucleus is nearly stable while a free neutron decays via the weak interaction with the life time of about 880 s, implies that the dominant, axial vector form factor or axial coupling constant  $g_A$ , in a nuclear medium is also to be modified and different from that in free space.

Thus, it is quite meaningful to investigate the change of the neutrino-induced reactions due to the modification of nucleon properties in a nuclear medium, in order to pin down the ambiguities inherent in the nucleon and/or nuclear structure on the interpretation of various neutrino reactions in the cosmos. For the study of the nuclear weak structure, one needs more refined nuclear models, because the nuclear reaction by the emitted neutrino energy from the PNS, whose energy range is less than 100 MeV, is sensitive on the collective motion of inside nucleons.

In our previous paper, we studied the medium effects on the neutrino reaction by charged current [16]. A large asymmetry between the neutrino and anti-neutrino reactions in a dense nuclear medium is predicted. In this study, we focus on the NC reaction with the density-dependent weak form factors estimated in the quark-meson-coupling model (QMC) [17–20]. The model has been successfully applied to study the properties of hadrons in nuclear matter, finite nuclei and hypernuclei [21–23]. For more through understanding of the medium effects

or the effects by the change of nucleon properties in a nuclear medium, the  $\nu_e$  and  $\bar{\nu}_e$  reactions on the nucleon in nuclear matter [24] as well as in  $^{12}\text{C}$  are examined in detail. Nuclear structure for  $^{12}\text{C}$  is treated by Quasi-particle RPA (QRPA) [25, 26].

This paper is organized as follows. Sec. II is devoted to explain the form factors used in this study. Detailed discussions regarding the form factors in dense matter and their numerical results are addressed in Appendix A and B. Numerical results for the neutrino reaction via NC on the nucleon in nuclear matter and  $^{12}\text{C}$  are presented in Sec. III. Summary and conclusions are given in Sec. IV.

## II. WEAK FORM FACTORS IN NUCLEAR WEAK CURRENT

By the standard electro-weak theory, the weak current operator  $W^\mu$  used for the  $\nu$ -induced reaction takes a  $V^\mu - A^\mu$  current form which has isoscalar and isovector parts for NC interaction [25]:

$$\begin{aligned} W^\mu &= V_3^\mu - A_3^\mu - 2\sin^2\theta_W J_{em}^\mu - \frac{1}{2}(V_s^\mu - A_s^\mu), \\ &= (1 - 2\sin^2\theta_W)V_3^\mu - A_3^\mu - 2\sin^2\theta_W V_0^\mu - \frac{1}{2}(V_s^\mu - A_s^\mu), \end{aligned} \quad (1)$$

with the Weinberg angle  $\theta_W$ . Here  $J_{em}^\mu = V_3^\mu + V_0^\mu$ , and  $V_3^\mu$  and  $A_3^\mu$  are plus components of the isovector  $V_i^\mu$  and  $A_i^\mu$  by the isospin rotation, *i.e.*  $V_3^\mu = V_{1+2i}^\mu$  and  $A_3^\mu = A_{1+2i}^\mu$ . Strangeness contributions, which are isoscalar parts, could be considered at  $-\frac{1}{2}(V_s^\mu - A_s^\mu)$ . For the charged current (CC) interaction, only  $V_3^\mu - A_3^\mu$  term is involved, so that the CC reaction is nearly independent of the strangeness content in a nucleon. For the elastic scattering of polarized electrons on the nucleon,  $J^\mu = -2\sin^2\theta_W J_{em}^\mu - \frac{1}{2}V_s^\mu$  is exploited, while only  $J_{em}^\mu = V_3^\mu + V_0^\mu$  is usually taken for the meson electro-production.

For a free nucleon, the weak current operator comprises the vector, the axial vector and the pseudo scalar form factors,  $F_i^V(Q^2)$ ,  $F_A(Q^2)$  and  $F_P(Q^2)$ :

$$W^\mu = F_1^V(Q^2)\gamma^\mu + F_2^V(Q^2)\frac{i}{2M_N}\sigma^{\mu\nu}q_\nu + F_A(Q^2)\gamma^\mu\gamma^5 + \frac{F_P(Q^2)}{2M}q^\mu\gamma^5. \quad (2)$$

Here we take the scalar form factor in the vectorial part and the axial tensor form factor in the axial part to be zero, because of the conservation of the vector current (CVC) and no existence of the second class current, respectively. By the CVC hypothesis with the inclusion

of the isoscalar strange quark contributions  $F_i^s(Q^2)$ , the vector form factors for protons and neutrons  $F_i^{V, p(n)}(Q^2)$  are expressed as [28]:

$$\begin{aligned} F_i^{V, p(n)(NC)} &= \left(\frac{1}{2} - 2 \sin^2 \theta_W\right) F_i^{p(n)}(Q^2) - \frac{1}{2} F_i^{n(p)}(Q^2) - \frac{1}{2} F_i^s(Q^2), \\ F_i^{V, p(n)(CC)} &= (F_i^p(Q^2) - F_i^n(Q^2)). \end{aligned} \quad (3)$$

The axial form factor is given by

$$F_A^{NC}(Q^2) = \frac{1}{2}(\mp g_A + g_A^s)/(1 + Q^2/M_A^2)^2, \quad F_A^{CC}(Q^2) = -g_A/(1 + Q^2/M_A^2)^2, \quad (4)$$

where  $g_A$  and  $M_A$  are the axial coupling constant and the axial cut off mass, respectively. The sign,  $-(+)$  comes from the isospin dependence of the target proton (neutron), respectively [29]. The axial form factor in Eq. (4) is just negative to the form factor elsewhere, for example, in Ref. [28], because we take the  $+$  sign for the  $F_A(Q^2)$  in Eq. (2). Although the ambiguity from the strangeness content in a nucleon still persists [31], the contribution to total cross section is less than 10 % even in the quasi-elastic region [27]. Therefore, we do not take the strangeness contribution into account in this work.

Before applying to the neutrino reaction, we need to figure out the change of nucleon properties in a nuclear medium, such as the effective nucleon mass, the axial coupling constant, the weak form factors of the nucleon. Those properties are calculated in the quark-meson coupling (QMC) model [17–20]. The constituent quark mass in a hadron is generated by the quark condensate,  $\langle \bar{q}q \rangle$ , in vacuum, but the mass (or  $\langle \bar{q}q \rangle$ ) in nuclear matter may be reduced from the value in vacuum because of the condensed scalar ( $\sigma$ ) field depending on the nuclear density  $\rho$ . The decrease of the quark mass then leads to the variation of baryon internal structures at the quark level. Such effect are considered self-consistently in the QMC model. Detailed features of the form factors and their modifications in nuclear matter used in this study are summarized in Appendix A and B.

In Fig. 1, effective nucleon mass in nuclear matter,  $M^*(\rho)$ , is illustrated, which shows a monotonic decrease with the increase of nuclear density. The modification of the axial vector form factor in nuclear matter is also shown in the right panel in Fig. 1 as a function of four momentum transfer  $Q^2[GeV/c]^2$ , which is normalized to that in free space,  $R(g_A) = g_A(\rho, Q^2)/g_A(\rho = 0, Q^2)$ . Even in the small momentum transfer region, where most of the neutrino reaction in the cosmos expected to occur, the reduction of the axial form factor  $g_A(\rho, Q^2)$  amounts to 11% around  $\rho = \rho_0$ . In the quasi-elastic region, the  $Q^2$  dependence

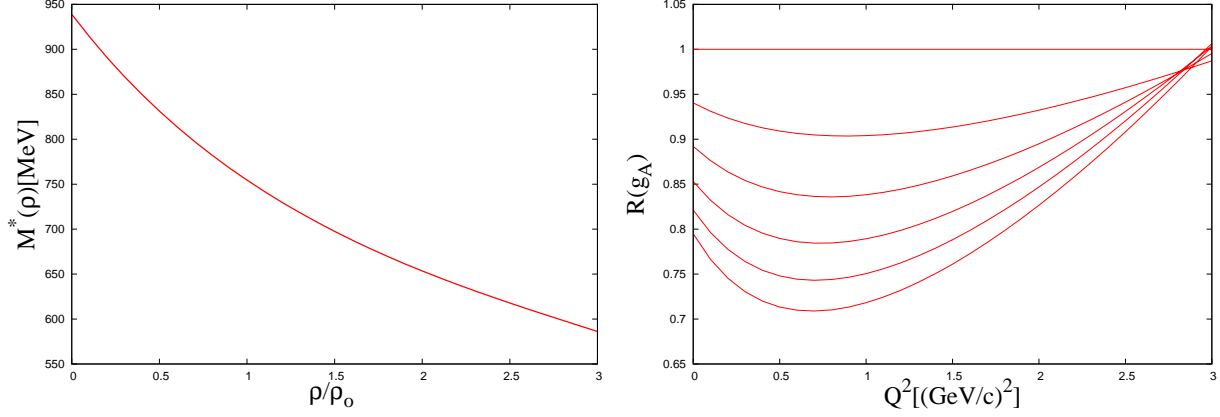


FIG. 1: (Color online) Effective nucleon mass  $M^*(\rho)$  presented in terms of the nuclear density ratio  $\rho/\rho_o$  (left), and the axial vector form factor normalized to that in free space (right),  $R(g_A) = g_A(\rho, Q^2)/g_A(\rho = 0, Q^2)$ , with finite momentum transfer in nuclear matter. From the uppermost (vacuum) in the right panel, the density ratio is increased by  $0.5 \rho_o$ . The lowermost curve is for  $\rho = 2.5\rho_o$ .

of the form factors on each density becomes more significant. Detailed discussions on the change of vector form factors in a nuclear medium adopted in this paper are summarized as figures in Appendix B.

### III. EFFECTS OF DENSITY DEPENDENT WEAK FORM FACTORS ON THE NEUTRINO REACTION VIA NC ON THE NUCLEON IN NUCLEAR MATTER AND $^{12}\text{C}$

#### A. Results on the Nucleon in Dense Matter

By using the following Sachs form factors and  $G_A^{NC} = F_A^{NC}$

$$G_E^V(Q^2) = F_1^V(Q^2) - \frac{Q^2}{4M^2}F_2^V(Q^2), \quad G_M^V(Q^2) = F_1^V(Q^2) + F_2^V(Q^2), \quad (5)$$

we calculated differential cross sections of the neutrino (antineutrino) reactions on the nucleon via NC as follows [31, 32]

$$\begin{aligned} \left(\frac{d\sigma}{dQ^2}\right)_{\nu(\bar{\nu})}^{NC} &= \frac{G_F^2}{2\pi} \left[ \frac{1}{2}y^2(G_M)^2 + \left(1 - y - \frac{M}{2E_\nu}y\right) \frac{(G_E)^2 + \frac{E_\nu}{2M}y(G_M)^2}{1 + \frac{E_\nu}{2M}y} \right. \\ &\quad \left. + \left(\frac{1}{2}y^2 + 1 - y + \frac{M}{2E_\nu}y\right)(G_A)^2 \mp 2y\left(1 - \frac{1}{2}y\right)G_M G_A \right], \end{aligned} \quad (6)$$

$$\left(\frac{d\sigma}{dQ^2}\right)_{\nu(\bar{\nu})}^{CC} = \left(\frac{d\sigma}{dQ^2}\right)_{\nu(\bar{\nu})}^{NC} (G_E \rightarrow G_E^{CC}, G_M \rightarrow G_M^{CC}, G_A \rightarrow G_A^{CC}),$$

with

$$G_E^{CC} = G_E^p(Q^2) - G_E^n(Q^2), \quad G_M^{CC} = G_M^p(Q^2) - G_M^n(Q^2). \quad (7)$$

Here we omit superscript 'V' for the form factors.  $E_\nu$  is the energy of the incident  $\nu(\bar{\nu})$  in the laboratory frame, and  $y = p \cdot q / p \cdot k = Q^2 / 2p \cdot k$  with  $k, p$  and  $q$  being respectively initial 4-momenta of  $\nu(\bar{\nu})$  and target nucleon, and 4-momentum transfer to the nucleon. The sign,  $- (+)$ , corresponds to the  $\nu (\bar{\nu})$ . Therefore, the difference and the sum of the cross sections are simply summarized as

$$\left(\frac{d\sigma}{dQ^2}\right)_{\nu}^{NC} - \left(\frac{d\sigma}{dQ^2}\right)_{\bar{\nu}}^{NC} = -\frac{G_F^2}{2\pi} 4y\left(1 - \frac{1}{2}y\right)G_M G_A, \quad (8)$$

$$\begin{aligned} \left(\frac{d\sigma}{dQ^2}\right)_{\nu}^{NC} + \left(\frac{d\sigma}{dQ^2}\right)_{\bar{\nu}}^{NC} &= \frac{G_F^2}{\pi} \left[ \frac{1}{2}y^2(G_M)^2 + \left(1 - y - \frac{M}{2E_\nu}y\right) \frac{(G_E)^2 + \frac{E_\nu}{2M}y(G_M)^2}{1 + \frac{E_\nu}{2M}y} \right. \\ &\quad \left. + \left(\frac{1}{2}y^2 + 1 - y + \frac{M}{2E_\nu}y\right)(G_A)^2 \right], \end{aligned} \quad (9)$$

and those via CC case are given by the replacements,  $G_E \rightarrow G_E^{CC}, G_M \rightarrow G_M^{CC}, G_A \rightarrow G_A^{CC}(= F_A^{CC})$  in Eqs. (8) and (9).

Numerical results obtained using the in-medium modified weak form factors are summarized in Fig. 2, where total cross sections for  $\bar{\nu}_e + p \rightarrow \bar{\nu}_e' + p$  (left) and  $\nu_e + n \rightarrow \nu_e' + n$  (right) via NC in nuclear matter are presented. Total cross sections decrease about 15% per each density increase step until the  $\rho \sim 2.5\rho_0$  (sky-blue (dot dashed) curve). However, for the  $\nu_e + n \rightarrow \nu_e' + n$  reaction, the variation in nuclear matter below  $E_\nu \sim 30$  MeV is less than 3%. Even the cross sections around  $E_\nu \sim 80$  MeV decrease about 12% maximally at  $\rho = \rho_0$  (blue (dotted) curve) compared to that in free space (black (solid) curve).

This large asymmetry for the  $\bar{\nu}_e$  and  $\nu_e$  reactions due to the change in the nucleon properties in a nuclear medium, which was also found in the CC reaction [16], can be understood by the last, helicity-dependent (HD) term in Eq. (6) in an analogous way to the CC case [16]. The HD term contribution can be estimated from the asymmetry in the neutrino reaction,  $\sigma^- = \sigma(\nu_e) - \sigma(\bar{\nu}_e)$ . For example, in Fig. 3, we plot the related cross sections,  $\sigma^-$  and  $\sigma^+ = \sigma(\nu_e) + \sigma(\bar{\nu}_e)$ , which respectively correspond to the HD and helicity independent (HID) term in Eq. (6). The HD term in the left panel shows the increase of



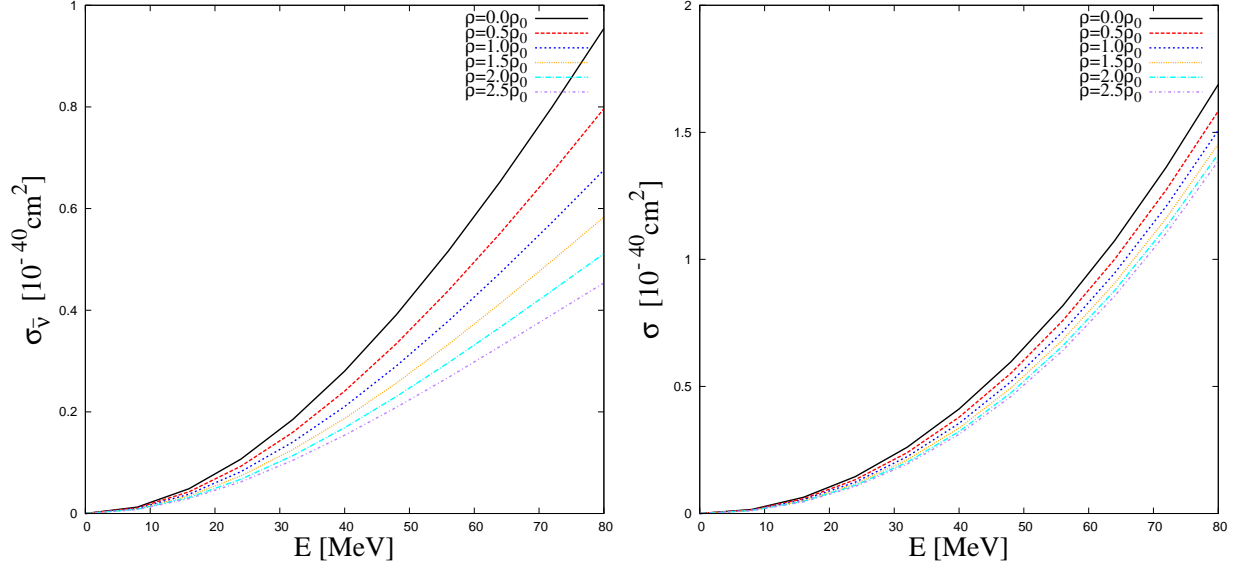


FIG. 2: (Color Online) Density dependence of the total cross sections for  $\bar{\nu}_e + p \rightarrow \bar{\nu}'_e + p$  (left) and  $\nu_e + n \rightarrow \nu'_e + n$  (right) in nuclear matter. The y axis is  $10^{-40} \text{ cm}^2$ , while the x-axis is the incident neutrino energy in MeV. Black (solid) curves are the results in free space. Cross sections decrease with increasing the density, by  $\rho/\rho_0 = 0.5$  (red (dashed)), 1.0 (blue (dotted)), 1.5 (yellow (short dotted)), 2.0 (sky-blue (dot long dashed)) and 2.5 (cyan (dot short dashed)) in both reactions.

the cross sections with increasing the nuclear density, while the HID term in the right panel shows the decrease of the cross sections with increasing the density.

For the  $\nu_e$  reaction, which is a half of the sum of  $\sigma^-$  and  $\sigma^+$  shown in the both panels, the HD term plays a countervailing role of the medium effects leading to the smaller effects, while the HD term enhances the medium effects for the  $\bar{\nu}_e$  reaction. Therefore, the large asymmetry between the  $\nu_e$  and  $\bar{\nu}_e$  reaction cross section comes from the different helicities of  $\nu$  and  $\bar{\nu}$ . Radiative corrections in the  $\nu_e$  reaction are not taken into account in this work, because the effects are known to be less than 2 % [33]. If we compare present NC results with those of the CC reaction in our preceding paper [16], this asymmetry can be arisen in the  $\nu$  reaction, irrespective of the current types.

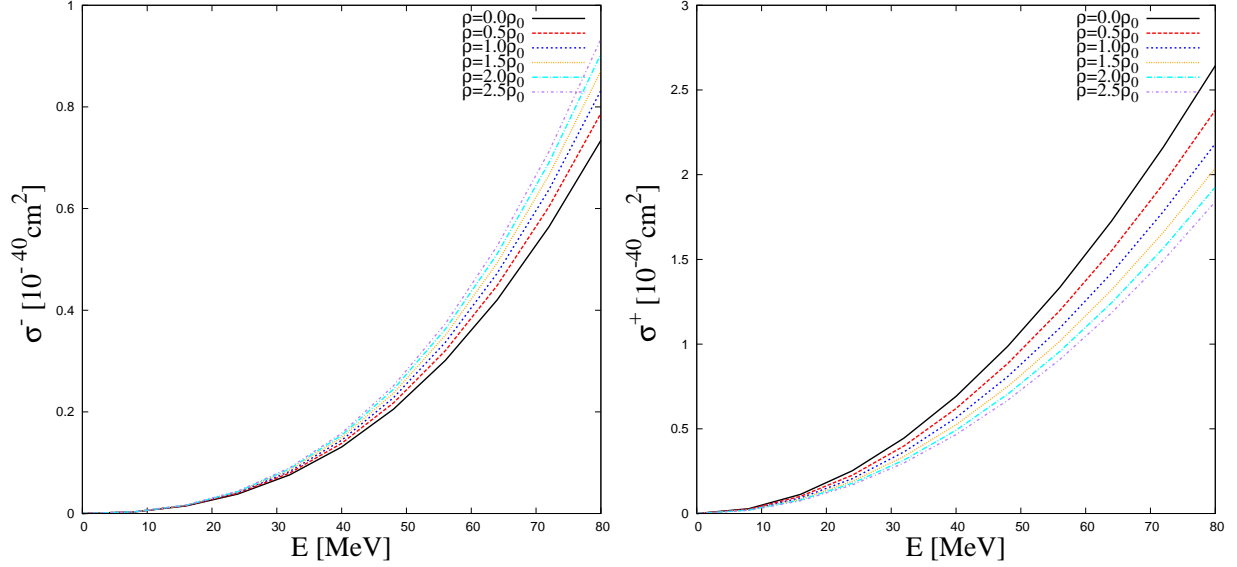


FIG. 3: (Color Online) Comparison of the total cross sections via the NC reaction for  $\sigma^- = \sigma(\nu_e) - \sigma(\bar{\nu}_e)$  (left) and  $\sigma^+ = \sigma(\nu_e) + \sigma(\bar{\nu}_e)$  (right), which respectively correspond to the HD and HID terms in Eq. (6). Legends for the curves are the same as those for Fig. 2.

### B. Results on the Bound Nucleon in $^{12}\text{C}$

To calculate the neutrino reaction on  $^{12}\text{C}$ , we use the following differential cross section formula, whose detailed explanations can be found in Ref. [25],

$$\begin{aligned}
 \left(\frac{d\sigma_\nu}{d\Omega}\right)_{(\nu/\bar{\nu})} &= \frac{G_F^2 \epsilon k}{\pi (2J_i + 1)} \left[ \sum_{J=0} (1 + \vec{v} \cdot \vec{\beta}) | \langle J_f | \hat{\mathcal{M}}_J | J_i \rangle |^2 \right. \\
 &+ (1 - \vec{v} \cdot \vec{\beta} + 2(\hat{v} \cdot \hat{q})(\hat{q} \cdot \vec{\beta})) | \langle J_f | \hat{\mathcal{L}}_J | J_i \rangle |^2 - \hat{q} \cdot (\hat{v} + \vec{\beta}) 2\text{Re} \langle J_f | \hat{\mathcal{L}}_J | J_i \rangle \langle J_f | \hat{\mathcal{M}}_J | J_i \rangle^* \\
 &+ \sum_{J=1} (1 - (\hat{v} \cdot \hat{q})(\hat{q} \cdot \vec{\beta})) (| \langle J_f | \hat{\mathcal{T}}_J^{el} | J_i \rangle |^2 + | \langle J_f | \hat{\mathcal{T}}_J^{mag} | J_i \rangle |^2) \\
 &\left. \pm \sum_{J=1} \hat{q} \cdot (\hat{v} - \vec{\beta}) 2\text{Re} [ \langle J_f | \hat{\mathcal{T}}_J^{mag} | J_i \rangle \langle J_f | \hat{\mathcal{T}}_J^{el} | J_i \rangle^* ] \right], \tag{10}
 \end{aligned}$$

where  $\vec{v}$  and  $\vec{k}$  are the 3-momenta of the incident and final neutrinos, and  $\vec{q} = \vec{k} - \vec{v}$ ,  $\vec{\beta} = \vec{k}/\epsilon$  with the final neutrino's energy  $\epsilon$ . Of course, the extremely relativistic limit (ERL) may yield more simple formula, but we use the general expression to get accurate results.

We have applied Eq. (10) to the  $^{12}\text{C}(\bar{\nu}_e, \nu'_e)^{12}\text{C}^*(1^+)$  and  $^{12}\text{C}(\nu_e, \nu'_e)^{12}\text{C}^*(1^+)$  reactions. The reactions can be treated by the  $\Delta J = 1$  transition from the  $0^+$  ground state of  $^{12}\text{C}$  to the  $1^+$  excited state. Descriptions of the nuclear states are performed by the QRPA framework [26]. Our numerical results are presented in Fig. 4. Medium effects on  $\bar{\nu}_e$  and  $\nu_e$  reactions on  $^{12}\text{C}$  appear in a similar fashion to those on the nucleon in nuclear matter.

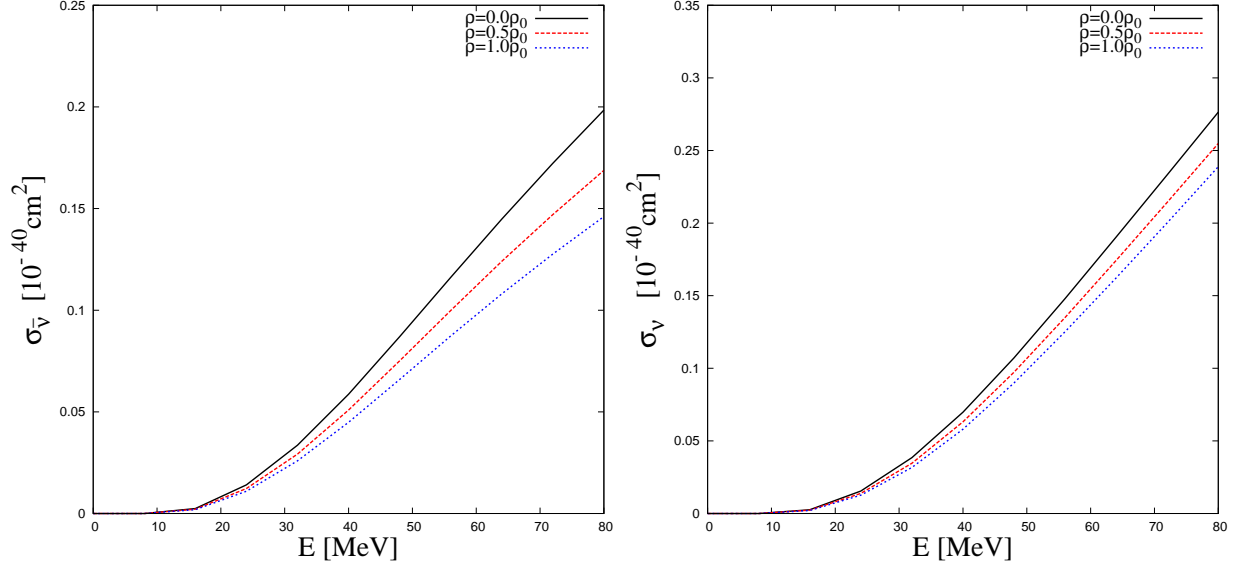


FIG. 4: (Color Online) Density dependence for the  $^{12}\text{C}(\bar{\nu}_e, \bar{\nu}'_e)^{12}\text{C}^*(1^+)$  (left) and  $^{12}\text{C}(\nu_e, \nu'_e)^{12}\text{C}^*(1^+)$  (right) reactions. The y axis is  $10^{-40}\text{cm}^2$ , while the x-axis is the incident neutrino energy in MeV. The cross sections decrease with increasing the nuclear density *i.e.*  $\rho/\rho_o = 0.5$  (red(dashed)) and  $1.0$  (blue(dotted)) in both reactions.

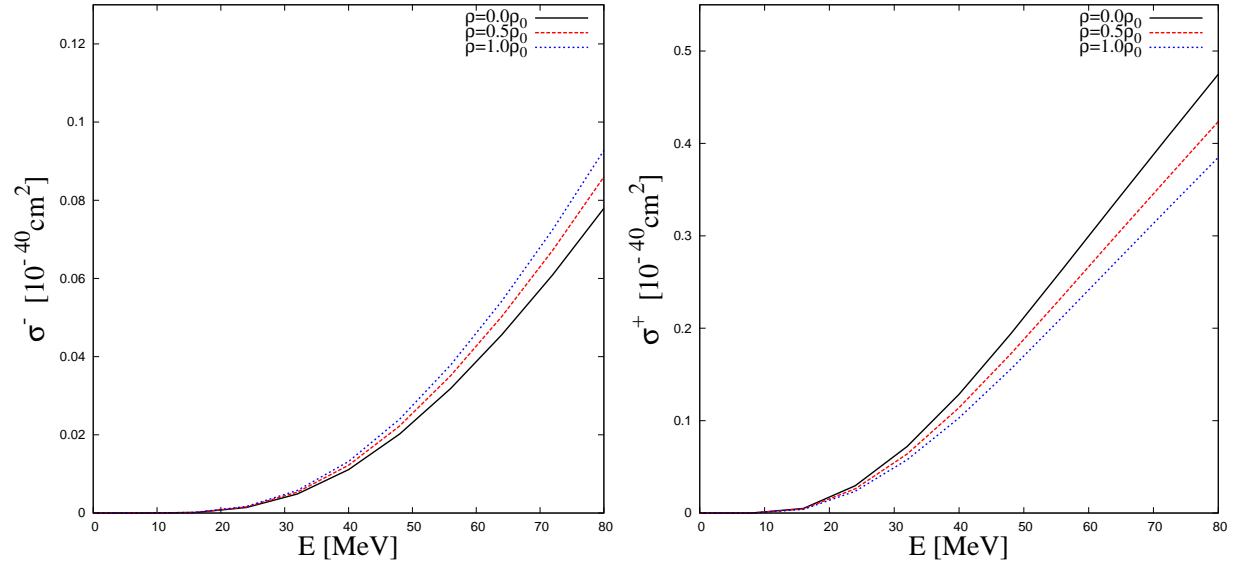


FIG. 5: (Color Online) Comparison of the total cross sections on  $^{12}\text{C}$  via the NC reaction for  $\sigma^- = \sigma(\nu_e) - \sigma(\bar{\nu}_e)$  (left) and  $\sigma^+ = \sigma(\nu_e) + \sigma(\bar{\nu}_e)$  (right), which correspond to the HD and the HID parts in Eq. (10). Legends for the curves are the same as those for Fig. 4.

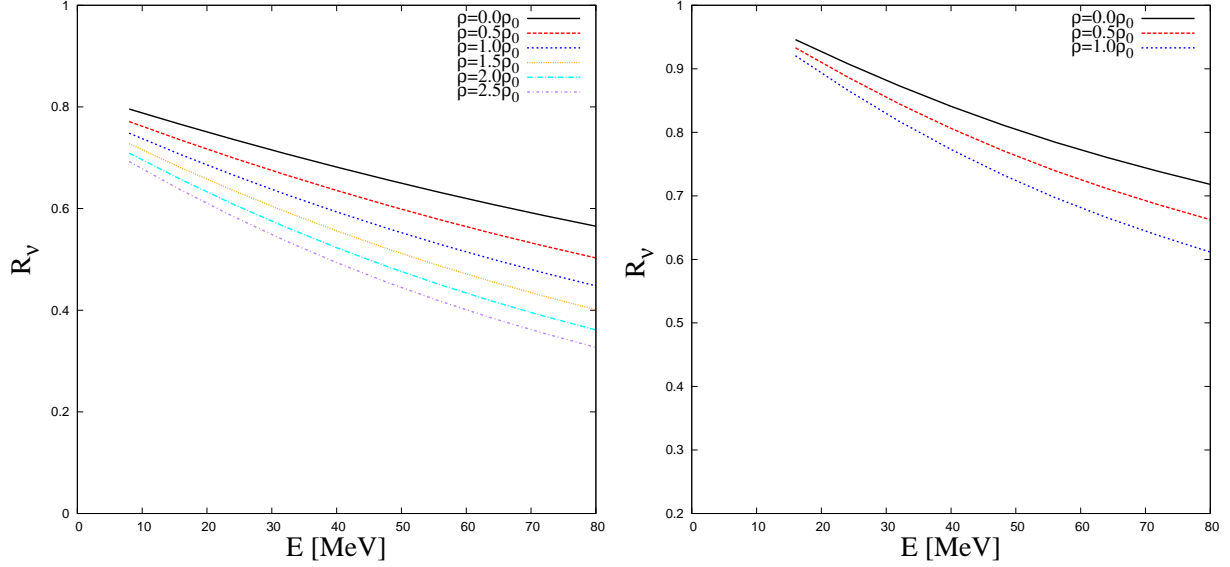


FIG. 6: (Color Online) Density and incident energy dependence of  $\bar{\nu}_e$  and  $\nu_e$  reaction (NC) ratio,  $R_\nu = \sigma(\bar{\nu}_e)/\sigma(\nu_e)$ , on the nucleon (left) and  $^{12}\text{C}$  (right), which are the cross section ratios of left and right panels in Figs.2 and 4, respectively. Legends for the curves are same as Fig.4.

Total cross sections for the  $\nu_e$  reaction decrease about 15% per each density decrease of  $0.5 \rho_o$ , while those for the  $\bar{\nu}_e$  reaction are about 5% for each decrease of the nuclear density. If we take the average Fermi momentum of the nucleon in  $^{12}\text{C}$ ,  $k_F = 225 \text{ MeV} (\rho = 0.668 \rho_o)$  [24], the maximum change by the in-medium effects is shown to be less than 7%. Since we consider the exclusive reaction for the ground state of daughter nuclei, the cross sections are smaller than those for the nucleon in Fig. 2.

In order to justify our approach to the NC neutrino reaction in finite nuclei, we compare our results to the experimental data,  $10.4 \pm 1.0 \pm 0.9 \times 10^{-42} \text{ cm}^2$ , which was measured as the flux averaged cross section of  $(\nu_e, \nu'_e) + (\nu_\mu, \nu'_\mu)$  reactions on  $^{12}\text{C}$  target [34]. If we take into account of the medium effect on  $^{12}\text{C}$  by adopting  $\rho = 0.6 \rho_o$ , our result become  $9.52 \times 10^{-42} \text{ cm}^2$  [25], which is consistent with the data. Comparison to the CC reactions data was done in Ref. [16].

In Fig.5, one may find that similar mechanism to the case of a nucleon in nuclear matter gives also rise to the asymmetry on the neutrino reaction on  $^{12}\text{C}$  in Fig.4. Namely the HD term, the last term in Eq.(10), calculated as  $\sigma^-$  in the left panel of Fig.5 enhances (supresses) the medium effects on the  $\bar{\nu}_e$  ( $\nu_e$ ) reaction. Finally, in Fig. 6, we show the cross section ratios,  $\sigma(\bar{\nu}_e)/\sigma(\nu_e)$ , on the nucleon in nuclear matter and  $^{12}\text{C}$ . All ratios decrease

with increasing the incident energy  $E_\nu$ . It would be a valuable low energy extension of the previous calculations performed beyond  $E_\nu = 100$  MeV region [35]. As for the medium effects, the higher the density increases, the smaller the ratios of the  $\bar{\nu}_e$  to the  $\nu_e$  reaction become. It means that the asymmetry between the  $\bar{\nu}_e$  and  $\nu_e$  reactions would be increased in a denser nuclear medium. More careful treatment of the  $\nu$  and  $\bar{\nu}$  propagation in dense matter are necessary for more thorough understanding of the phenomena related to the neutrino propagation in nuclear matter.

#### IV. SUMMARY

In summary, we applied the bound nucleon weak form factors modified in a nuclear medium to the neutrino and the anti-neutrino reactions via neutral current on the nucleon in nuclear matter and  $^{12}\text{C}$ . The form factors are calculated in the QMC model, and retain explicitly the four-momentum transfer and the density dependence. Anti-neutrino reaction cross sections are largely suppressed in nuclear matter, i.e., about 30 % maximal suppression around  $\rho = \rho_0$  similarly to that observed for the CC reaction. However, the neutrino cross sections in dense matter may be modified about 12 ~ 18 %, maximally. Such asymmetry turns out to appear irrespective of the target. Therefore, it could affect significantly the neutrino scattering, in particular, the anti-neutrino propagation inside the proto-neutron star.

Recent neutrino facilities present lots of fruitful data for the neutrino reaction in the quasi-elastic region [36, 37]. Although most of the data are now focused on the extraction of the axial mass and the strangeness content on a nucleon by the quasi-elastic kinematics, the study of the asymmetry between the neutrino and anti-neutrino reactions by more data on the  $\bar{\nu}$  reaction could be the valuable alternative approach to understand the modification of the nucleon properties in a nuclear medium.

#### Acknowledgments

This work was supported by the National Research Foundation of Korea (Grant No. 2011-0003188). The work of KT was supported by the University of Adelaide and the Australian

Research Council through grant No. FL0992247 (Anthony William Thomas).

---

- [1] T. Fischer, I. Sagert, G. Pagliara, M. Hempel, J. Schaffner-Bielich, T. Rauscher, F.-K. Thielemann, R. Kaeppli, G. Martinez-Pinedo, and M. Liebendoerfer, *Astrophys. J. Supplement* **194**, 39 (2011).
- [2] Tomoyuki Maruyama, Toshitaka Kajino, Nobutoshi Yasutake, Myung-Ki Cheoun, Chung-Yeol Ryu, *Phys. Rev. D* **83**, 081303 (2011).
- [3] Tomoyuki Maruyama, Nobutoshi Yasutake, Myung-Ki Cheoun, Jun Hidaka, Toshitaka Kajino, Grant J. Mathews, Chung-Yeol Ryu, *Phys. Rev. D* **86**, 123003 (2012).
- [4] Tomoyuki Maruyama, Jun Hidaka, T. Kajino, Nobutoshi Yasutake, T. Kuroda, Myung-Ki Cheoun, Chung-Yeol Ryu, Grant J. Mathews, arXiv:1301.7495[astro-ph.SR] (2013).
- [5] Shinya Wanajo, Hans-Thomas Janka, Shigeru Kubono, *Astrophys. J.* **729**, 46 (2011).
- [6] Myung-Ki Cheoun, Eunja Ha, T. Hayakawa, Toshitaka Kajino, Satoshi Chiba, *Phys. Rev.* **C82**, 035504 (2010).
- [7] Myung-Ki Cheoun, Eunja Ha, T. Hayakawa, Satoshi Chiba, Ko Nakamura, Toshitaka Kajino, Grant J. Mathews, *Phys. Rev.* **C85**, 065807 (2012).
- [8] T. Yoshida, T. Suzuki, S. Chiba, T. Kajino, H. Yokomukura, K. Kimura, A. Takamura, H. Hartmann, *Astrophys. J.* **686**, 448 (2008).
- [9] S. Malov, K. Wijesooriya, F. T. Baker, L. Bimbot, E. J. Brash, C. C. Chang, J. M. Finn, K. G. Fissum et al., *Phys. Rev. C* **62**, 057302 (2000).
- [10] S. Dieterich, P. Bartsch, D. Baumann, J. Bermuth, K. Bohinc, R. Bohm, D. Bosnar, S. Derber et al., *Phys. Lett. B* **500**, 47-52 (2001).
- [11] S. Strauch et al. [ Jefferson Lab E93-049 Collaboration ], *Phys. Rev. Lett.* **91**, 052301 (2003).
- [12] M. Paolone, S. P. Malace, S. Strauch, I. Albayrak, J. Arrington, B. L. Berman, E. J. Brash, B. Briscoe et al., *Phys. Rev. Lett.* **105**, 072001 (2010).
- [13] S. P. Malace, M. Paolone, S. Strauch, I. Albayrak, J. Arrington, B. L. Berman, E. J. Brash, B. Briscoe et al., *Phys. Rev. Lett.* **106**, 052501 (2011).
- [14] For a review, W. K. Brooks, S. Strauch and K. Tsushima, *J. Phys. Conf. Ser.* **299**, 012011 (2011).
- [15] I. C. Cloet, G. A. Miller, E. Piasetzky and G. Ron, *Phys. Rev. Lett.* **103**, 082301 (2009).

- [16] Myung-Ki Cheoun, Ki-Seok Choi, K.S. Kim, Koichi Saito, Toshitaka Kajino, Kazuo Tsushima and Tomoyuki Maruyama, arXiv:1302.5770 [nucl-th], (2013).
- [17] D. -H. Lu, K. Tsushima, A. W. Thomas, A. G. Williams and K. Saito, Phys. Rev. C **60**, 068201 (1999).
- [18] D. -H. Lu, K. Tsushima, A. W. Thomas, A. G. Williams and K. Saito, Phys. Lett. B **441**, 27 (1998).
- [19] D. -H. Lu, A. W. Thomas, K. Tsushima, A. G. Williams and K. Saito, Phys. Lett. B **417**, 217 (1998).
- [20] D. -H. Lu, A. W. Thomas and K. Tsushima, nucl-th/0112001 (2011).
- [21] K. Saito, K. Tsushima and A. W. Thomas, Nucl. Phys. A **609**, 339 (1996):  
K. Saito, K. Tsushima and A. W. Thomas, Phys. Rev. C **55**, 2637 (1997).
- [22] K. Tsushima, K. Saito, J. Haidenbauer and A. W. Thomas, Nucl. Phys. A **630**, 691 (1998):  
P. A. M. Guichon, A. W. Thomas and K. Tsushima, Nucl. Phys. A **814**, 66 (2008):  
K. Tsushima and F. C. Khanna, Phys. Rev. C **67**, 015211 (2003):  
K. Tsushima and F. C. Khanna, J. Phys. G **30**, 1765 (2004).
- [23] K. Saito, K. Tsushima and A. W. Thomas, Prog. Part. Nucl. Phys. **58**, 1 (2007).
- [24] K. Tsushima, Hungchong Kim, and K. Saito, Phys. Rev. C **70**, 038501 (2004).
- [25] Myung-Ki Cheoun, Eunja Ha, K.S. Kim, Toshitaka Kajino, J. Phys. G **37**, 055101 (2010).
- [26] Myung-Ki Cheoun, Eunja Ha, Su Youn Lee, K.S. Kim, W.Y. So, Toshitaka Kajino, Phys. Rev. C **81**, 028501 (2010).
- [27] Myung-Ki Cheoun and K.S. Kim, J. Phys. G **35**, 065107 (2008).
- [28] Andrea Meucci, Carlotta Giusti, and Franco Davide Pacati, Nucl. Phys. **A739**, 277 (2004);  
Nucl. Phys. **A744**, 307 (2004); Nucl. Phys. **A773**, 250 (2006).
- [29] M. J. Musolf and T. W. Donnelly, Nucl. Phys. **A546**, 509 (1992).
- [30] Hungchong Kim, J. Piekarewicz and C. J. Horowitz, Phys. Rev. C **51**, 2739(1995).
- [31] Myung-Ki Cheoun and K.S. Kim, J. Phys. G **35**, 065107 (2008).
- [32] W. M. Alberico, S. M. Bilenky, C. Maieron, Phys. Rep. **358**, 227-308, (2002).
- [33] Alessandro Strumia and Francesco Vissani, Phys. Lett. B **564**, 42 (2003).
- [34] C. Athanassopoulos et al. (LSND Collaboration), Phys. Rev. C **55**, 2078 (1997).
- [35] K. S. Kuzmin, V. V. Lyubushkin, and V. A. Naumov, Physics of Atomic Nuclei **69**, 1857 (2006).

- [36] A. A. Aguilar-Arevalo et. al (MiniBooNE Collaboration), Phys. Rev. **D** 81, 092005 (2010).
- [37] A. A. Aguilar-Arevalo et. al (MiniBooNE Collaboration), Phys. Rev. **D** 82, 092005 (2010).
- [38] N. Paar, D. Vretenar, T. Marketin and P. Ring, Phys. Rev. **C** 77, 024608 (2008).
- [39] T. W. Donnelly and J. D. Walecka, Phys. Rev. **C** 6, 719 (1972).
- [40] J. D. Walecka, *Muon Physics*, edited by V. W. Hughes and C. S. Wu, (Academic Press, New York, 1975).
- [41] T. Ericson and W. Weise, *Pions and Nuclei*, (CLARENDON PRESS, Oxford, 1988).



## Appendix A: Definitions of Form Factors

In this paper, we use two different nucleon form factors. One is the Sachs form factors based on the dipole form factor [29, 30]:

$$G_D^V(Q^2) \equiv (1 + Q^2/M_V^2)^{-2} = (1 + 4.97 \tau)^{-2} = G_E^{p,emp}(Q^2), \quad (A1)$$

$$G_E^{n,emp}(Q^2) = -\mu_n \tau G_D^V(Q^2) \eta, \quad G_M^{p,emp}(Q^2) = \mu_p G_D^V(Q^2), \quad G_M^{n,emp}(Q^2) = \mu_n G_D^V(Q^2),$$

where  $q = k_\nu^i - k_\nu^f = p_f - p_i, q^2 (= -Q^2) = q_0^2 (= \omega^2) - \mathbf{q}^2 \leq 0$  with  $\tau = Q^2/(4M_N^0)^2 = -q^2/(4M_N^0)^2 \geq 0, \eta = (1 + 5.6 \tau)^{-1}$  and  $M_N^0 = 0.939, \mu_p (= 1 + \lambda_p) = 2.793, \mu_n (= \lambda_n) = -1.913$ .

Note the following facts.

1) The  $Q^2 = \omega^2 - \mathbf{q}^2$  defined in Eq. (24) in Ref. [29] is correct, but the argument  $Q^2$  in the form factors is understood as  $|Q^2|$  as shown in their figures. In the same sense, the  $G_D^V \equiv (1 - Q^2/M_V^2)^{-2}$  in Eq. (33c) is correct, *i.e.*  $G_D^V \equiv (1 - |Q^2|/M_V^2)^{-2}$ . But it should be rewritten as  $G_D^V \equiv (1 + Q^2/M_V^2)^{-2}$  by our notation  $Q^2 = \mathbf{q}^2 - \omega^2$ .

2) Since  $Q^2/M_V^2 = 4.97 \tau = 4.97 Q^2/(4M_N^0)^2$ ,  $M_V^2$  is 0.71 GeV<sup>2</sup> ( $M_V = 0.84$  GeV), which is consistent with the standard value [41].

The Sachs form factors are related to the Dirac and Pauli form factors as follows

$$F_1^{p,emp}(Q^2) = (G_E^{p,emp}(Q^2) + \tau G_M^{p,emp}(Q^2))/(1 + \tau) = [1 + \tau(1 + \lambda_p)]G_D^V(Q^2)/(1 + \tau),$$

$$F_1^{n,emp}(Q^2) = (G_E^{n,emp}(Q^2) + \tau G_M^{n,emp}(Q^2))/(1 + \tau) = \tau \lambda_n (1 - \eta) G_D^V(Q^2)/(1 + \tau),$$

$$F_2^{p,emp}(Q^2) = (G_M^{p,emp}(Q^2) - G_E^{p,emp}(Q^2))/(1 + \tau) = \lambda_p G_D^V(Q^2)/(1 + \tau),$$

$$F_2^{n,emp}(Q^2) = (G_M^{n,emp}(Q^2) - G_E^{n,emp}(Q^2))/(1 + \tau) = \lambda_n (1 + \tau \eta) G_D^V(Q^2)/(1 + \tau), \quad (A2)$$

vice verse

$$G_E^{p(n),emp}(Q^2) = F_1^{p(n),emp}(Q^2) - \tau F_2^{p(n),emp}(Q^2), \quad G_M^{p(n),emp}(Q^2) = F_1^{p(n),emp}(Q^2) + F_2^{p(n),emp}(Q^2). \quad (A3)$$

The isovector-vector weak form factors are given by the Dirac and Pauli form factors,

$$F_{1,2}^V(Q^2) = F_{1,2}^{p,emp}(Q^2) - F_{1,2}^{n,emp}(Q^2) \quad (CC), \quad (A4)$$

$$F_{1,2}^{V,p(n)}(Q^2) = \left(\frac{1}{2} - 2 \sin^2 \theta_w\right) F_{1,2}^{p(n)}(Q^2) - \frac{1}{2} F_{1,2}^{n(p)}(Q^2) \quad (NC),$$

where the NC case is taken from our previous paper [25] and Ref. [28]. On the other hand, the axial vector form factor is given by  $G_A^{emp} = g_A^{cc} \times (1 + Q^2/M_A^2)^{-2}$  with  $M_A = 1.03$  GeV and  $g_A = 1.26$ .

Other form factors introduced in Refs. [38–40] are all assumed to have the same momentum dependence in MeV units:

$$\begin{aligned}
F_1^V(q^2) &= (1 + q^2/(855\text{MeV})^2)^{-2}, \quad F_A(q^2) = -1.23 \times (1 + q^2/(855\text{MeV})^2)^{-2}, \quad (\text{A5}) \\
\mu_V(q^2) &= F_1^V(q^2) + 2M_N F_2^V(q^2) = 4.706 \times (1 + q^2/(855\text{MeV})^2)^{-2}, \\
F_P(q^2) &= 2M_N F_A(q^2)/(q^2 + m_\pi^2),
\end{aligned}$$

with  $m_\pi = 139.57$  MeV,  $M_N = 931.49432$  MeV,  $\mu_V(0) = \mu_p - \mu_n = 4.706$ .

Note the following facts.

1) Here  $q^2 = \mathbf{q}^2 - q_0^2$  defined by Eq. (80) in Ref. [40] is the same  $Q^2$  definition with our notation. The  $F_1^V(q^2)$  in A(5) is almost same as that in (A4) because  $F_1^V(q^2) = F_1^p(Q^2) - F_1^n(Q^2) \simeq G_D^V(q^2) = (1 + Q^2/(855\text{MeV})^2)^{-2}$  in the low momentum transfer region. But,  $F_A(q^2)$  is a bit different from the standard one, *i.e.*  $M_A = 0.855$  GeV and  $g_A = -1.23$  in (A5) is smaller than  $M_A = 1.03$  GeV and  $g_A = 1.26$ , where the “minus” sign comes from the different sign in the axial part of the weak current.

2) If we define  $2M_N F_2^V(q^2) = F_2^V(q^2)$  which depends on the definition of the vector current,  $\mu_V(q^2)$  in (A5) is equal to  $G_M^V(q^2)$  in Eq.(5) because  $\mu_V(q^2) = F_1^V(q^2) + F_2^V(q^2) \simeq (1 + \lambda_p - \lambda_n)G_D^V(q^2) = (\mu_p - \mu_n)G_D^V(q^2) = 4.706 \times (1 + q^2/(855\text{MeV})^2)^{-2}$  in the low momentum transfer region.

## Appendix B: Density dependent Form Factors

Here, we show the density dependence of the various form factors calculated in the QMC model. In Figs. 7-10,  $G_E^p(\rho, Q^2)$ ,  $G_E^n(\rho, Q^2)$ ,  $G_M^p(\rho, Q^2)$  and  $G_M^n(\rho, Q^2)$  form factors and their ratios  $R(G_{E,M}^{p,n}) = G_{E,M}^{p,n}(\rho, Q^2)/G_{E,M}^{p,n}(\rho = 0, Q^2)$  are presented. Ratios of the electric form factors in Figs. 7 and 8 converge to 1.0 at  $Q^2 = 0$ , but those of the magnetic form factors in Figs. 9 and 10 are enhanced. The axial vector form factor is quenched in a nuclear medium, even at  $Q^2 = 0$ , which causes the change of the neutrino reaction in dense matter in the cosmos, albeit their small momentum transfer. Ratios of density-dependent weak form factors,  $F_{1,2}^V$ , are presented in Fig. 12. About a 25 % increase of  $F_2^V$  is to be noticed for the weak interaction in dense matter.

But in the neutrino reaction on the quasi-elastic region, for example, the kinematical region performed at MiniBooNE experiments [36, 37], the dependence on the 4-momentum transfer  $Q^2$ , as well as that on the nuclear density, may be practically important.

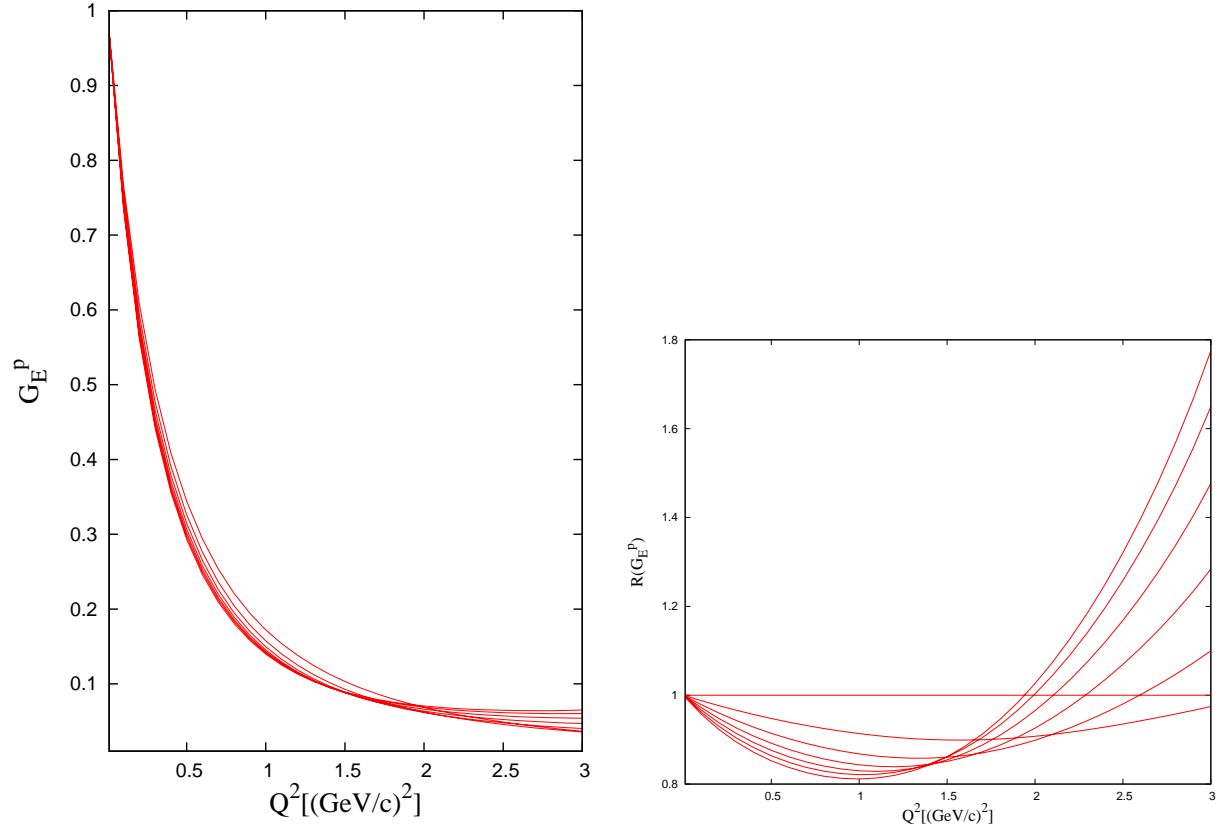


FIG. 7: (Color online)  $G_E^p(\rho, Q^2)$  and  $R(G_E^p) = G_E^p(\rho, Q^2)/G_E^p(\rho = 0, Q^2)$  in nuclear matter. The uppermost curves at  $Q^2 = 1.5 [\text{GeV}/c]^2$  are for  $\rho = 0$ , from which density increases by  $0.5 \rho_0$ .

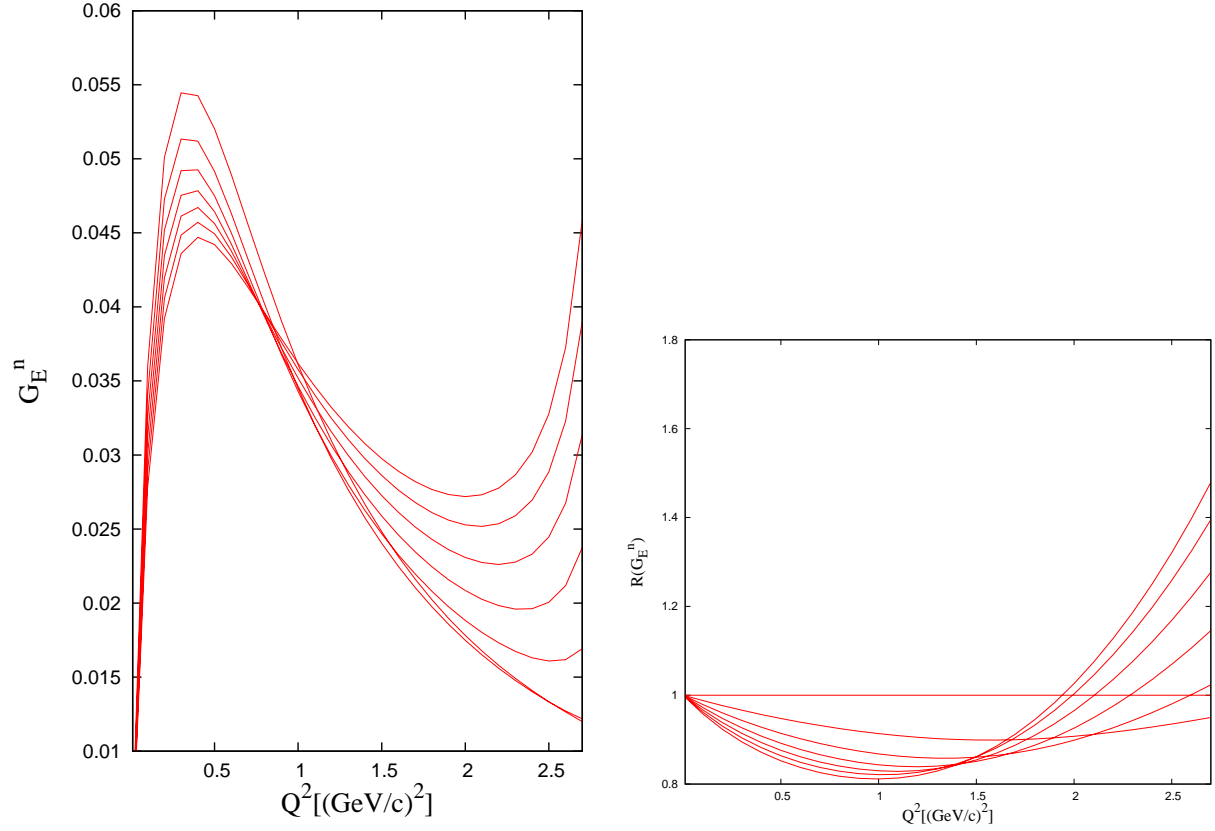


FIG. 8: (Color online)  $G_E^n(\rho, Q^2)$  and  $R(G_E^n) = G_E^n(\rho, Q^2)/G_E^n(\rho = 0, Q^2)$  in nuclear matter. The uppermost curves at  $Q^2 = 0.5 \text{ [GeV/c]}^2$  are for  $\rho = 0$ , from which density increases by  $0.5 \rho_0$ .

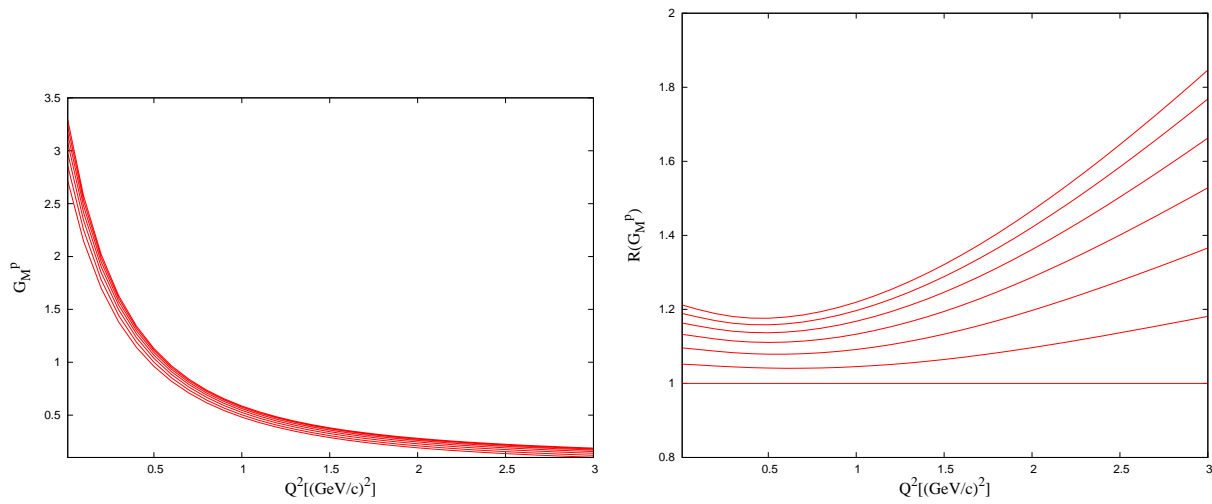


FIG. 9: (Color online)  $G_M^p(\rho, Q^2)$  and  $R(G_M^p) = G_M^p(\rho, Q^2)/G_M^p(\rho = 0, Q^2)$  in nuclear matter. The lowermost curves are for  $\rho = 0$ , from which density increases by  $0.5 \rho_0$ .

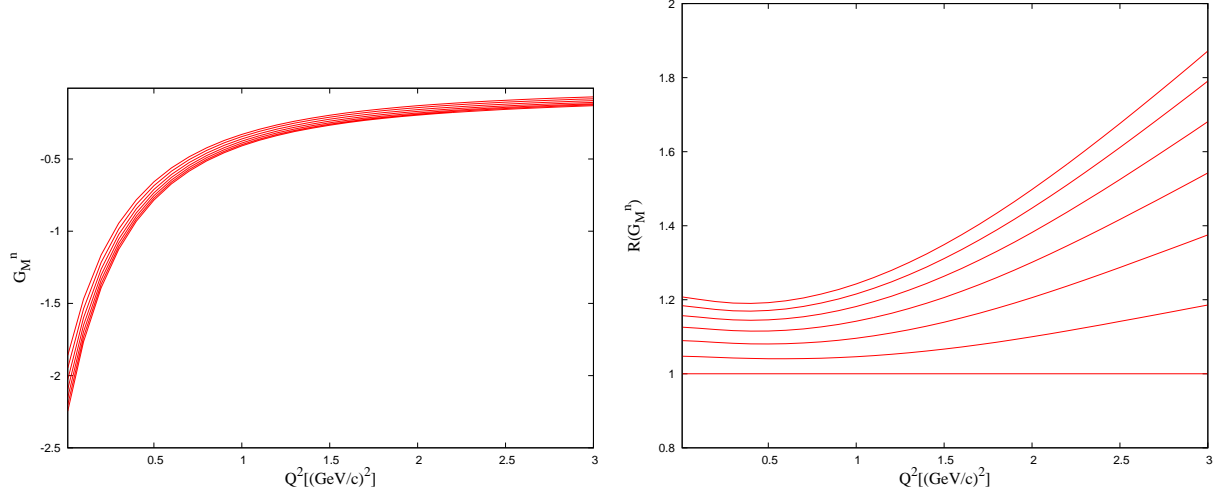


FIG. 10: (Color online)  $G_M^n(\rho, Q^2)$  and  $R(G_M^n) = G_M^n(\rho, Q^2)/G_M^n(\rho = 0, Q^2)$  in nuclear matter. The uppermost (lowermost) curve in left (right) is for  $\rho = 0$ , from which density is increases by  $0.5 \rho_0$ .

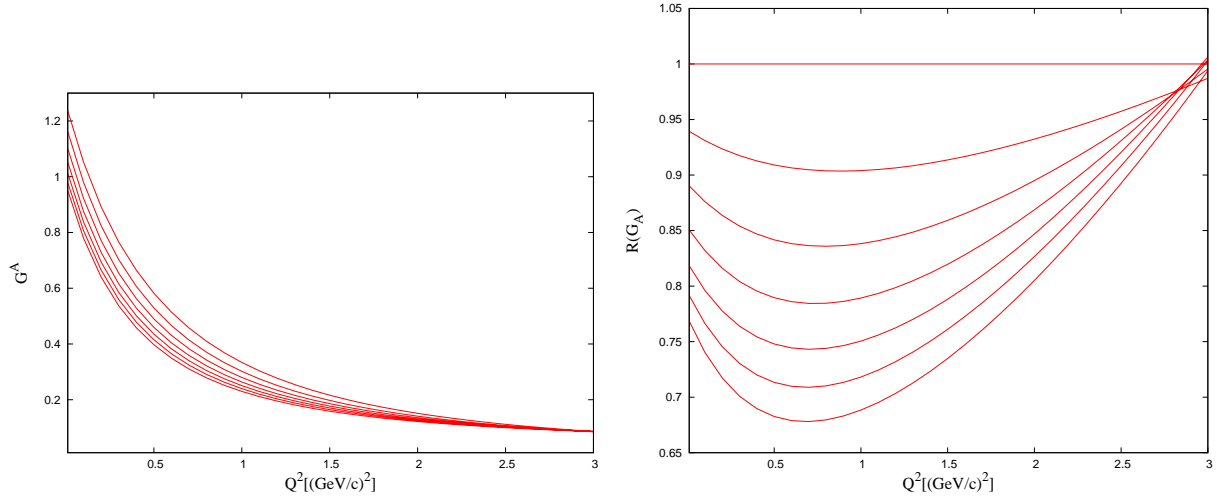


FIG. 11: (Color online)  $G_A(\rho, Q^2)$  and  $R(G_A) = G_A(\rho, Q^2)/G_A(\rho = 0, Q^2)$  in nuclear matter. The uppermost curves are for  $\rho = 0$ , from which density increases by  $0.5 \rho_0$ .

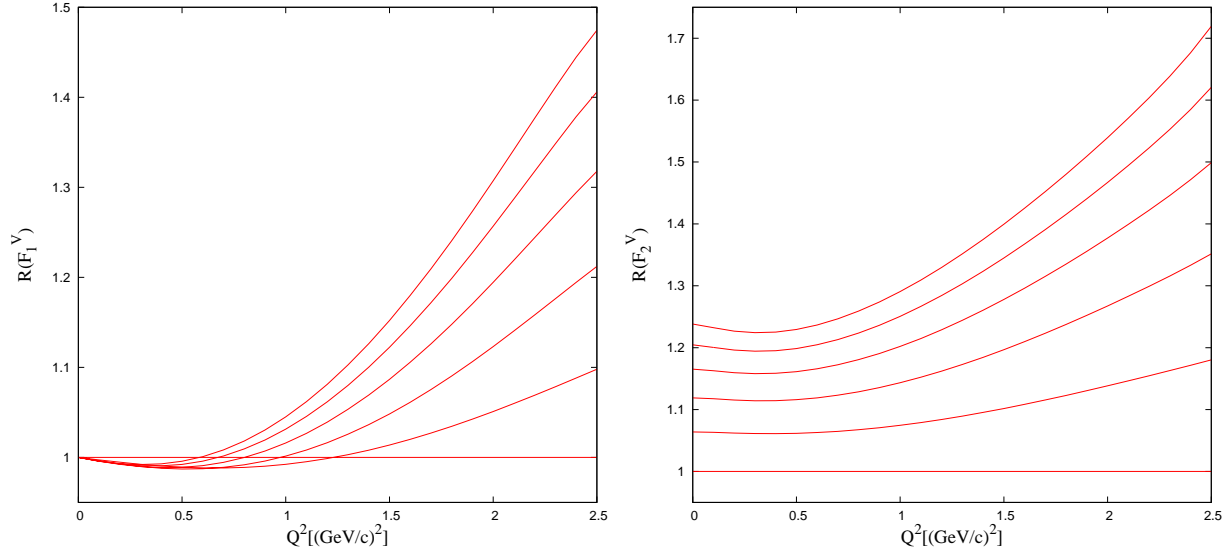


FIG. 12: Modification in the weak vector form factors,  $R(F_{1,2}^V) = F_{1,2}^V(\rho, Q^2)/F_{1,2}^V(\rho = 0, Q^2)$ , with finite momentum transfer in nuclear matter. From the lowermost (vacuum), density ratios increase by  $0.5 \rho_0$ . The uppermost curve is for  $\rho = 2.5\rho_0$ .